

# Impacts of direct release and river discharge on oceanic $^{137}\text{Cs}$ derived from the Fukushima Dai-ichi Nuclear Power Plant accident

Daisuke Tsumune <sup>a,\*</sup>, Takaki Tsubono <sup>a</sup>, Kazuhiro Misumi <sup>a</sup>, Yutaka Tateda <sup>a</sup>, Yasushi Toyoda <sup>a</sup>, Yuichi Onda <sup>b</sup>, Michio Aoyama <sup>b</sup>

<sup>a</sup> Environmental Science Research Laboratory, Central Research Institute of Electric Power Industry, 1646, Abiko, 270-1194, Japan

<sup>b</sup> Faculty of Life and Environmental Sciences, Univ. of Tsukuba, 305-8577, Japan

## ARTICLE INFO

**Keywords:**  
Fukushima Dai-ichi nuclear power plant accident  
Radiocaesium  
Regional ocean model  
Direct release  
River discharge

## ABSTRACT

A series of accidents at the Fukushima Dai-ichi Nuclear Power Plant (1F NPP) following the Great East Japan Earthquake and tsunami of 11 March 2011 resulted in the release of radioactive materials to the ocean. We used the Regional Ocean Model System (ROMS) to simulate the  $^{137}\text{Cs}$  activity in the oceanic area off Fukushima, with the sources of radioactivity being direct release, atmospheric deposition, river discharge, and inflow across the domain boundary. The direct release rate of  $^{137}\text{Cs}$  after the accident until the end of 2016 was estimated by comparing simulated results with measured  $^{137}\text{Cs}$  activities adjacent to the 1F NPP. River discharge rates of  $^{137}\text{Cs}$  were estimated by multiplying simulated river flow rates by the dissolved  $^{137}\text{Cs}$  activities, which were estimated by an empirical function. Inflow of  $^{137}\text{Cs}$  across the domain boundary was set according to the results of a North Pacific Ocean model. Because the spatiotemporal variability of  $^{137}\text{Cs}$  activity was large, the simulated results were compared with the annual averaged observed  $^{137}\text{Cs}$  activity distribution. Normalized annual averaged  $^{137}\text{Cs}$  activity distributions in the regional ocean were similar for each year from 2013 to 2016. This result suggests that the annual averaged distribution is predictable. Simulated  $^{137}\text{Cs}$  activity attributable to direct release was in good agreement with measurement data from the coastal zone adjacent to the 1F NPP. Comparison of the simulated results with measured activity in the offshore area indicated that the simulation slightly underestimated the activity attributable to inflow across the domain boundary. This result suggests that recirculation of subducted  $^{137}\text{Cs}$  to the surface layer was underestimated by the North Pacific model. During the study period, the effect of river discharge on oceanic  $^{137}\text{Cs}$  activity was small compared to the effect of directly released  $^{137}\text{Cs}$ .

## 1. Introduction

A series of accidents at the Fukushima Dai-ichi Nuclear Power Plant (1F NPP) following the Great East Japan Earthquake and tsunami of 11 March 2011 resulted in the release of radioactive materials to the ocean by two major pathways, direct release from the accident site and atmospheric deposition. Another possible release pathway is river discharge, and in the regional ocean, the flux across the regional boundary is also important, because atmospheric deposition occurred over the entire North Pacific Ocean.

Direct release rates have been estimated by several methods, but mainly by comparing measured  $^{137}\text{Cs}$  activity with activity simulated by numerical models (Estournel et al., 2012; Miyazawa et al., 2013; Tsumune et al., 2012, 2013). In studies conducted soon after the accident, the estimated results of total amount of direct release showed large

variation (0.94–27 PBq) (Masumoto et al., 2012; Tsumune et al., 2013), but in later investigations the variation was smaller (3–6 PBq) (Aoyama et al., 2016; Kumamoto et al., 2019). These uncertainties in the estimated total amount of direct release are due to the difficulty in distinguishing between the effects of atmospheric deposition and direct release on the measured  $^{137}\text{Cs}$  activity. The  $^{131}\text{I}/^{137}\text{Cs}$  activity ratio is useful for differentiating between these two release pathways (Tsumune et al., 2012), because in the case of direct release, this ratio is expected to decrease only as a result of the decay of  $^{131}\text{I}$ , which has a half-life of 8 days. In contrast, in the case of atmospheric deposition, changes in the  $^{131}\text{I}/^{137}\text{Cs}$  activity ratio reflect the different transport and deposition processes affecting  $^{131}\text{I}$ , which is present as a gas or as small particles, and  $^{137}\text{Cs}$ , which is present as larger particles. Tsumune et al. (2012) estimated that the total amount of directly released  $^{137}\text{Cs}$  was  $3.5 \pm 0.7$  PBq at the end of May 2011. Similarly, using the inverse method and an

\* Corresponding author.

E-mail address: [tsumune@criepi.denken.or.jp](mailto:tsumune@criepi.denken.or.jp) (D. Tsumune).

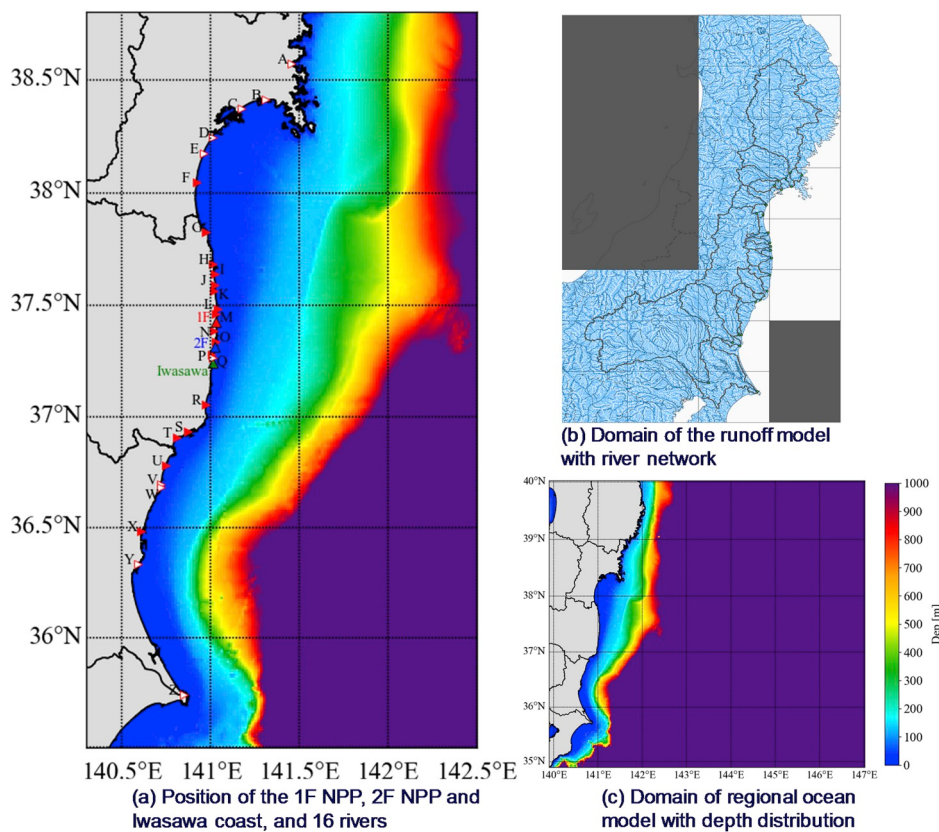


**Fig. 1.** (a) Positions of the 1F NPP, 2F NPP, the Iwasawa coast, and the mouths of 26 rivers (A, Kitakami; B, Kyu-Kitakami; C, Naruse; D, Nakakita; E, Natori; F, Abukuma; G, Uda; H, Mano; I, Niida; J, Ota; K, Odaka; L, Ukedo; M, Maeda; N, Kuma; O, Tomioka; P, Ide; Q, Kido; R, Natsui; S, Fujiwara; T, Same; U, Okita; V, Hananuki; W, Jyuo; X, Kuji; Y, Naka; and Z, Tone). Domains of (b) the river runoff model, showing the river network grey lines outline the individual river catchments, and (c) the regional ocean model, showing the depth distribution. The river network in (b) is based on 1:200,000 Topographic Maps provided by the Geospatial Information Authority of Japan.

ocean model, Estournel et al. (2012) estimated that the total amount of directly released  $^{137}\text{Cs}$  was 4.1–4.5 PBq from 12 March to 30 June 2011. Then, to reduce the bias in the representation of the measured  $^{137}\text{Cs}$  activity 30 km offshore, they added 1 PBq to their estimate, and the final estimated value was 5.1–5.5 PBq. The bias in the simulated  $^{137}\text{Cs}$  activity 30 km offshore may have been due to the lack of consideration of atmospheric deposition. The atmospheric deposition rate of  $^{137}\text{Cs}$  onto the ocean at a regional scale was still unknown because of the lack of measurement data. The results of inter-comparisons among regional atmospheric transport models also showed large uncertainties in the simulated atmospheric deposition of  $^{137}\text{Cs}$  on the regional ocean (Science Council of Japan, 2014). Tokyo Electric Power Company (TEPCO) calculated the flow rate of contaminated water from the hole in the wall of inlet canal of reactor 2 to be  $4.3 \text{ m}^3 \text{ h}^{-1}$  by using visual estimates of the distance, height, and diameter of the flow, and TEPCO measured the  $^{137}\text{Cs}$  activity of the contaminated water to be  $1.8 \times 10^{12} \text{ Bq m}^{-3}$  (Japanese Government, 2011). TEPCO then multiplied the calculated flow rate by the measured  $^{137}\text{Cs}$  activity of the contaminated water and estimated the direct release rate from 2 to 6 April 2011 to be  $1.9 \times 10^{14} \text{ Bq day}^{-1}$ . This value is similar to the value of  $2.2 \times 10^{14} \text{ Bq day}^{-1}$  estimated by Tsumune et al. (2013) at the same period. Kanda (2013) estimated the direct release rate of  $^{137}\text{Cs}$  from the estimated exchange rate of seawater and the measured  $^{137}\text{Cs}$  activity within the 1F NPP harbour to be  $9.3 \times 10^{10} \text{ Bq day}^{-1}$  in summer 2011 and  $8.1 \times 10^9 \text{ Bq day}^{-1}$  in summer 2012. Kanda (2013) pointed out that the direct release was continuous through September 2012 because the measured  $^{137}\text{Cs}$  activity continued to be higher adjacent to the 1F NPP compared with that in the surrounding area and with that before the 1F NPP accident. Machida et al. (2019) used the same method as Kanda (2013) to estimate the direct release rate through June 2018. In addition, Maderich et al. (2014, 2018) used a box model approach, rather than fine-scale numerical modelling, to conduct long-term simulations of  $^{137}\text{Cs}$  activity in the north-western Pacific.

Kitamura et al. (2014) estimated the discharge rate of  $^{137}\text{Cs}$  from

rivers to the ocean by numerical modelling. In river water,  $^{137}\text{Cs}$  occurs mainly in particulate form, but particulate  $^{137}\text{Cs}$  discharged to the ocean sinks immediately to the seabed (Kakehi et al., 2015); thus, the dissolved  $^{137}\text{Cs}$  discharge is more important in investigations of the effect of river discharge on oceanic  $^{137}\text{Cs}$  activity. Although recent studies have started to focus on dissolved  $^{137}\text{Cs}$  in rivers (Tsujii et al., 2016; Nakanishi and Sakuma, 2019; Taniguchi et al., 2019), owing to the large temporal changes in oceanic  $^{137}\text{Cs}$  activity and the continued direct release from the 1F NPP site, the amount of dissolved  $^{137}\text{Cs}$  supplied to the ocean from rivers is still unknown.

Another source for a regional-scale ocean model is the inflow of  $^{137}\text{Cs}$  initially deposited outside of the model domain. Tsumune et al. (2013) estimated the contribution of such inflow on  $^{137}\text{Cs}$  activity in the regional ocean from the North Pacific model results (Tsubono et al., 2016) and found that one year after the 1F NPP accident the effect of the inflow of  $^{137}\text{Cs}$  derived from the 1F NPP accident was negligible (Tsumune et al., 2013), and that after the first year inflow of  $^{137}\text{Cs}$  derived from the atmospheric nuclear weapons test was dominant.

In this study, the direct release rate was estimated to the end of 2016. In addition, river discharge rates from 16 rivers during 2013–2016 were empirically estimated by using simulated river flow rates and estimated dissolved  $^{137}\text{Cs}$  activities in the rivers (Taniguchi et al., 2019) (there were insufficient measurement data from the rivers for 2012 and earlier). Inflow across the domain boundary of the regional ocean model was obtained from the North Pacific Model results (Tsubono et al., 2016). We conducted regional ocean model simulations to investigate the effects on the surface  $^{137}\text{Cs}$  distribution in the regional ocean of direct release and cross-boundary inflow from March 2011 to December 2016, and of river discharge from January 2013 to December 2016. We examined the effects on the surface distribution only, because we did not have enough observation data on the vertical distribution of  $^{137}\text{Cs}$  activity. During the study period, there was large variation in the  $^{137}\text{Cs}$  distribution off the Fukushima coast caused by synoptic-scale wind fluctuations and, in the Kuroshio-Oyashio mixed water region,

mesoscale eddies. Therefore, we calculated annually averaged  $^{137}\text{Cs}$  distributions to investigate the effects of direct release, across-boundary inflow, and river discharge on the  $^{137}\text{Cs}$  distribution. We ignored  $^{137}\text{Cs}$  fluxes due to groundwater discharge and desorption from bottom sediment because data for the whole region included in this study were too few to estimate these fluxes.

## 2. Method

### 2.1. Ocean model

We used the Regional Ocean Modelling System (ROMS) (Shchepetkin and McWilliams, 2005) to simulate ocean dispersion of  $^{137}\text{Cs}$  released from the 1F NPP reactors off Fukushima. Model settings were similar to those used previously (Tsumune et al., 2013). The model represented the reasonable distribution of  $^{137}\text{Cs}$  up to February 2012. The objectives of this study were to investigate the effect of riverine input and to extend the simulation period to the end of 2016 by the previous model. The ROMS is a three-dimensional Boussinesq free-surface ocean circulation model formulated using terrain-following coordinates. In this study, the model domain covered the oceanic area off Fukushima ( $35^{\circ}54'\text{N}$ – $40^{\circ}00'\text{N}$ ,  $139^{\circ}54'\text{E}$ – $147^{\circ}00'\text{E}$ ) (Fig. 1(c)), and the horizontal resolution was set to  $1/120^{\circ}$  (about 1 km) in both zonal and meridional directions because a fine-scale model is necessary to represent submesoscale mixing (Kamidaira et al., 2018). The vertical resolution of the  $\sigma$  coordinate was 30 layers. The ocean bottom was set at a depth of 1,000 m to reduce the computer resources needed for the simulation. The model was forced at the sea surface by wind stress and by heat and freshwater fluxes, the values of which were acquired by a real-time nested simulation system (Numerical Weather Forecasting and Analysis System (NuWFAS); Hashimoto et al., 2010) of the Weather Research and Forecasting Model (WRF) (Skamarock et al., 2008), a global spectral model used for numerical weather prediction by the Japan Meteorological Agency (JMA). The horizontal resolution of this system was 5 km in both the zonal and meridional directions, and the time step of the output from the real-time simulation system was 1 h.

During the simulation, horizontal currents, temperature, salinity, and sea surface height along the open boundary were restored to the Japan Coastal Ocean Prediction Experiment 2 (JCOPE2) reanalysis data (Miyazawa et al., 2009), which have a horizontal resolution of  $1/10^{\circ}$ . To represent mesoscale eddies during the simulation period, temperature and salinity in the higher resolution ( $1/120^{\circ}$ ) ROMS were nudged to the JCOPE2 reanalysis results without coastal zone where the depth is less than 150 m to simulate the effect of the freshwater flux from rivers. As a strong constraint on the representation of mesoscale eddies and the Kuroshio Current, the nudging parameter was set at  $1 \text{ day}^{-1}$ . In the initial conditions, temperature, salinity, horizontal current velocities, and sea surface height were set by using the JCOPE2 reanalysis output. We modelled  $^{137}\text{Cs}$  as a passive tracer whose movement into the ocean interior was controlled by advection and diffusion. We assumed that the  $^{137}\text{Cs}$  activity in seawater decreased as a result of radioactive decay with a half-life of 30.1 years.

### 2.2. Estimation of the direct release rate

The direct release rate of  $^{137}\text{Cs}$  was estimated by comparing simulated results with  $^{137}\text{Cs}$  activities measured adjacent to the 1F NPP site (at the discharge from units 5 and 6 and from the south discharge canals) (Tsumune et al., 2012, 2013),

$$[\text{Direct release rate } (\text{Bq day}^{-1})]$$

$$= [\text{Measured } ^{137}\text{Cs activity } (\text{Bq m}^{-3})]$$

$$/ [\text{Simulated } ^{137}\text{Cs activity with unit release } (1 \text{ Bq day}^{-1}) \text{ in the release mesh } (\text{Bq m}^{-3}) / (\text{Bq day}^{-1})]$$

We employed  $^{137}\text{Cs}$  activities measured adjacent to the 1F NPP site once per week by TEPCO by the ammonium molybdate phosphate method (Aoyama and Hirose, 2008) which has a low detection limit (<http://www.tepco.co.jp/en/nu/fukushima-np/f1/smp/index-e.html>). The  $^{137}\text{Cs}$  activity was measured at two points along the coast, the discharge from units 5 and 6 (i.e., the 5,6 discharge) and south discharge canals, whereas the area of the release mesh used in the  $^{137}\text{Cs}$  simulation was about  $1 \text{ km} \times 1 \text{ km}$  and included the 1F NPP harbour. The presence of the harbour caused the dilution of  $^{137}\text{Cs}$  in the release mesh area (about  $1 \text{ km} \times 1 \text{ km}$ ) of the actual ocean to be enhanced. Therefore,  $^{137}\text{Cs}$  activities measured at these sampling points were used to represent the activity in the release mesh area. Where there is no harbour, a simulation with a finer mesh might be necessary to estimate the direct release from the measured  $^{137}\text{Cs}$  activities along the coast. Because of oceanic current changes, measured  $^{137}\text{Cs}$  activities varied over 3–4 days along the Fukushima coast. Therefore, a curve fitted to  $^{137}\text{Cs}$  activities measured over a period of more than 1 week was suitable for the estimation. The simulated  $^{137}\text{Cs}$  activities per unit release ( $(\text{Bq m}^{-3}) / (\text{Bq day}^{-1})$ ) were acquired from the results of the ROMS. The direct release rate is thus proportional to the curve fitted measured  $^{137}\text{Cs}$  activities adjacent to the 1F NPP.

### 2.3. Estimation of the river discharge rate

Because our focus was on the effects of river discharge on oceanic  $^{137}\text{Cs}$ , we calculated the river discharge rate of dissolved  $^{137}\text{Cs}$  by multiplying the river flow rate by the dissolved  $^{137}\text{Cs}$  activity in the river.

#### 2.3.1. River flow rates

River flow rates were calculated by applying a distributed runoff analysis model to the basins of 26 rivers (listed in Fig. 1(a)) around the 1F NPP. The runoff analysis model used for the river network (Fig. 1(b)), which has a horizontal resolution of  $1 \text{ km} \times 1 \text{ km}$ , considers the vegetation distribution and land use in each mesh (Toyoda and Hirakuchi, 2009), calculates the water balance between rainfall and runoff, and performs radiation and heat balance calculations to estimate evapotranspiration. In this study, meteorological data such as precipitation input into the model to use for the atmospheric driving force were obtained by interpolating the JMA reanalysis data. Interception evaporation in forest areas was calculated by using a vegetation tank model. The amount of snowmelt water (snowmelt tank) was calculated by using the snowmelt components of the radiation balance, sensible heat, latent heat, rainwater, and geothermal. A three-stage tank model was used to model underground flow: surface layer, unsaturated zone, and saturated zone. A one-dimensional kinematic wave model was used to model flow in river channels.

#### 2.3.2. $^{137}\text{Cs}$ activity in rivers

We employed the following empirical equation to estimate the dissolved  $^{137}\text{Cs}$  activity in each river (Taniguchi et al., 2019).

$$C_d(t) = \frac{DBe^{-\lambda t}}{K_d} \quad (1)$$

where  $C_d(t)$  is the dissolved  $^{137}\text{Cs}$  activity ( $\text{Bq m}^{-3}$ );  $t$  is time (year);  $D$  is the  $^{137}\text{Cs}$  inventory ( $\text{Bq m}^{-2}$ ) in the catchment area;  $B$  is a coefficient that differs for each river;  $\lambda$  is the exponential decay constant; and  $K_d$  is the distribution coefficient. Taniguchi et al. (2019) used different values of  $\lambda$  for the first (between June 2011 and March 2012) and second (between April 2012 and August 2015) periods. We used the second value from 2013 to 2016 because the period March to May 2011 was not included in the first period. We thus set  $\lambda$  to 0.29 (apparent half-life of 2.4 years) to estimate the dissolved  $^{137}\text{Cs}$  activity in the rivers. We used  $K_d = 2 \times 10^5 \text{ (Bq kg}^{-1}\text{)} / (\text{Bq L}^{-1})$  from the values in Taniguchi et al. (2019) to adjust the observed dissolved  $^{137}\text{Cs}$  activity in rivers shown

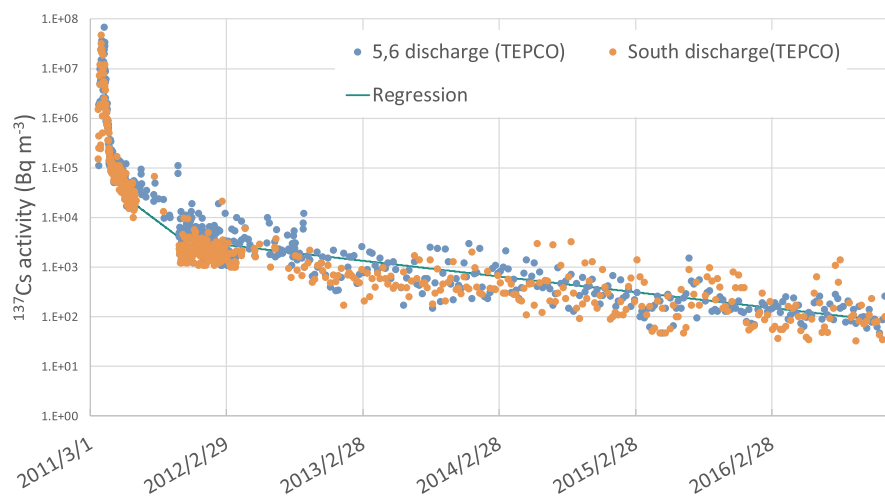


**Fig. 2.** Measured  $^{137}\text{Cs}$  activity adjacent to the 1F NPP site (at the 5,6 discharge and south discharge canals).

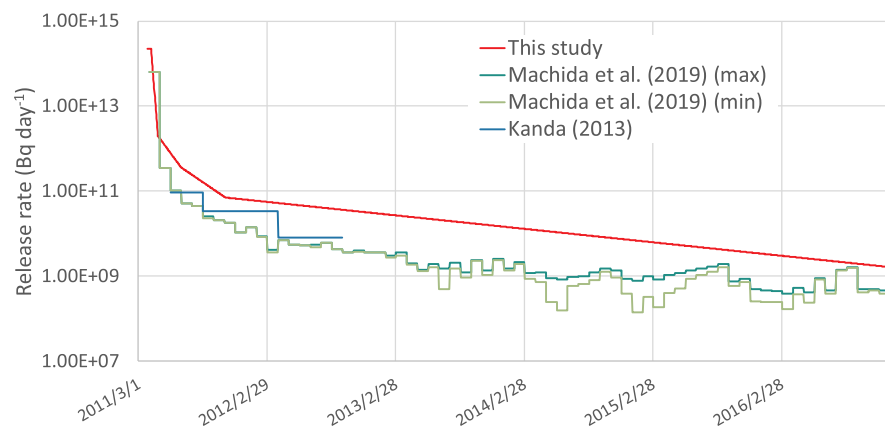


**Fig. 3.** The direct release rate curve estimated in this study and by Kanda (2013) and Machida et al. (2019).

later (Fig. 4). We used  $^{137}\text{Cs}$  inventories in catchment areas estimated by aerial monitoring by the Nuclear Regulation Authority (NRA) (Sanada et al., 2018). We estimated the dissolved  $^{137}\text{Cs}$  activity of 16 rivers (Abukuma, Uda, Mano, Niida, Ota, Odaka, Ukedo, Maeda, Kuma, Tomioka, Ide, Natsui, Fujiwara, Same, Okita, and Kuji; Fig. 1(a)) because the  $^{137}\text{Cs}$  deposition amount was very small in the basins of the other 10 rivers. We estimated the dissolved  $^{137}\text{Cs}$  activity in these 16 rivers from 2013 to 2016 to investigate the effects of riverine input on  $^{137}\text{Cs}$  activity in the ocean. The supplied  $^{137}\text{Cs}$  was immediately transported out of the simulation area, therefore riverine input before 2013 was not affected  $^{137}\text{Cs}$  activity in the ocean after 2013.

#### 2.4. Current measurement

The ocean current was measured by an Acoustic Doppler Current Profiler (ADCP; 600 Hz, RDI) from 8 October to 10 December 2014 and from 22 April to 25 June 2015, at a point about 5 km south and 2.8 km offshore from the 1F NPP ( $37^{\circ}22.6'\text{N}$ ,  $141^{\circ}3.7'\text{E}$ ). The ADCP was set on the seafloor at a water depth of 21 m.

### 3. Results and discussion

#### 3.1. Direct release rate

Fig. 2 shows measured  $^{137}\text{Cs}$  activities adjacent to the 1F NPP (at the

5,6 discharge and south discharge canals). By analysing the  $^{131}\text{I}/^{137}\text{Cs}$  activity ratio, Tsumune et al. (2012) estimated that direct release started on 26 March 2011. They attributed the measured  $^{137}\text{Cs}$  activity before then to atmospheric deposition because the  $^{131}\text{I}/^{137}\text{Cs}$  activity ratio was variable (see Section 1). The  $^{137}\text{Cs}$  activity increased on 26 March 2011 with the start of direct release and decreased on 6 April 2011, when visible release ceased following the injection of water glass (an aqueous sodium silicate solution) into a pit near reactor 2 (Japanese Government, 2011). The rate of decrease corresponded to the exchange rate of water in the harbour (Kanda, 2013), which was estimated to be 0.44 day $^{-1}$ . On a shorter timescale (3–4 days),  $^{137}\text{Cs}$  activity varied over one order of magnitude because of oceanic current changes. After November 2011, the  $^{137}\text{Cs}$  activity continued to decrease exponentially at same  $\lambda$  value ( $\lambda = 0.73$ ). The  $^{137}\text{Cs}$  activity  $C$  (Bq m $^{-3}$ ) due to direct release is expressed by the following equation:

$$C(t) = 3.5 \times 10^3 e^{(-0.73t)} \quad (2)$$

where  $t$  is time (year). The apparent half-life was 346 days.

The direct release rate of  $^{137}\text{Cs}$  is proportional to the exponential fitting curve of the measured  $^{137}\text{Cs}$  activity adjacent to the 1F NPP. Therefore, the direct release rate  $F$  (Bq day $^{-1}$ ) is expressed by the following equation:

$$F(t) = \frac{1}{5.0 \times 10^{-8}} C(t) \quad (3)$$

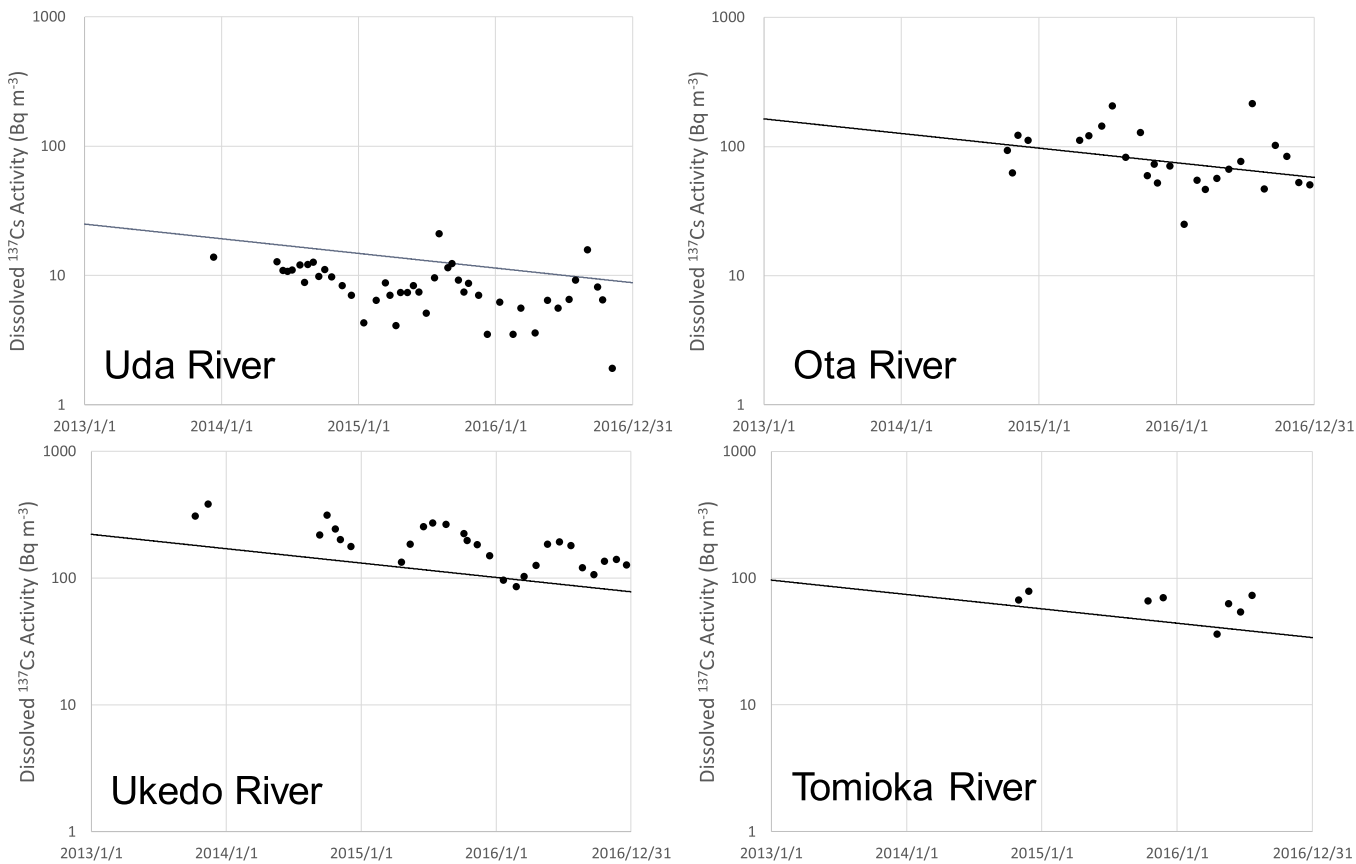


**Fig. 4.** Measure (points) and estimated (lines)  $^{137}\text{Cs}$  activity in rivers (Uda, Ota, Ukedo, and Tomioka).

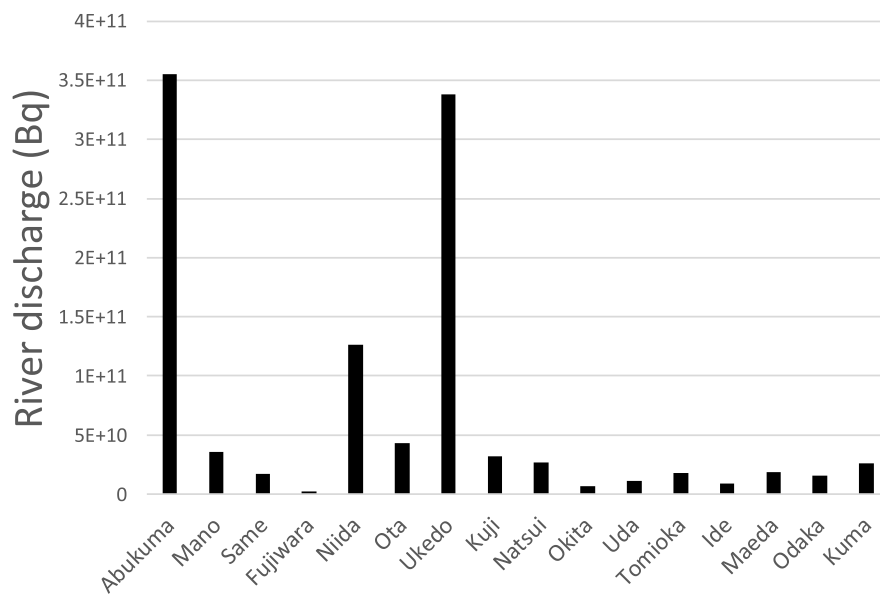


**Fig. 5.** Total amount of  $^{137}\text{Cs}$  discharge from 16 rivers around the 1F NPP from 2013 to 2016.

Fig. 3 shows the estimated direct release rate curve for 26 March 2011 to 31 December 2016 (Table S1) along with estimates by [Kanda \(2013\)](#) (June 2011 to September 2012) and [Machida et al. \(2019\)](#) (April 2011 to December 2016). In the early period, the direct release rate of  $^{137}\text{Cs}$  was estimated to be  $2.2 \times 10^{14} \text{ Bq day}^{-1}$ , and it decreased exponentially with time, reaching  $3.9 \times 10^9 \text{ Bq day}^{-1}$  by the end of 2016. The

estimated total amount of directly released  $^{137}\text{Cs}$  from 26 March 2011 to 31 December 2016 was  $3.6 \pm 0.7 \text{ PBq}$ . [Tsumune et al. \(2013\)](#) also estimated the total amount of directly released  $^{137}\text{Cs}$  to be  $3.6 \pm 0.7 \text{ PBq}$  during the first year after the accident. Thus, the continuing direct release did not increase the total amount of  $^{137}\text{Cs}$  released by the end of 2016. [Machida et al. \(2019\)](#) used Kanda's method ([Kanda, 2013](#); see

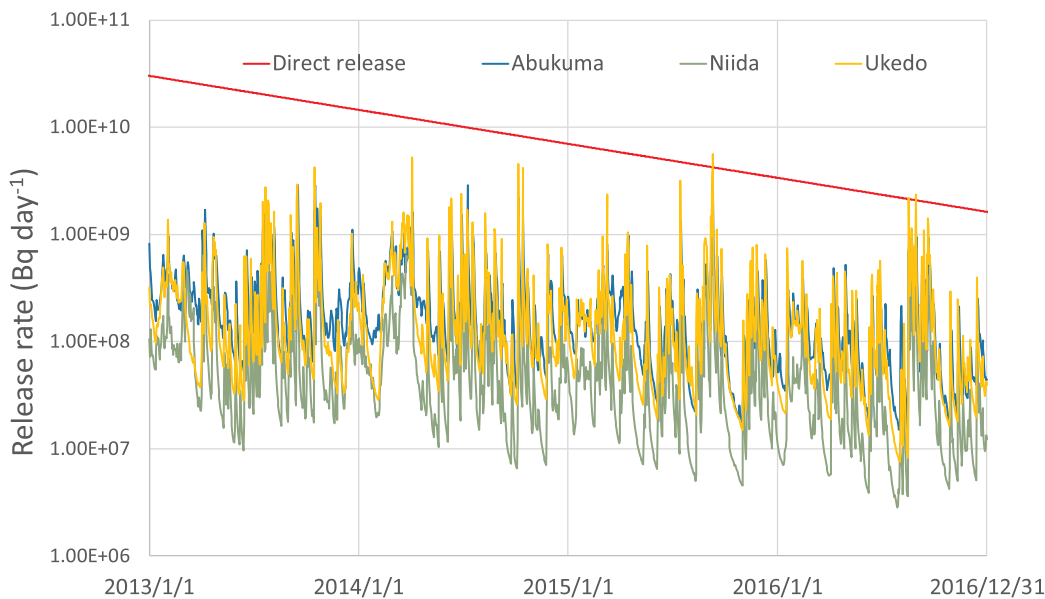


**Fig. 6.** Estimated dissolved  $^{137}\text{Cs}$  discharge rates from three major rivers, the Abukuma, Niida, and Ukedo rivers and the direct release rate from the 1F NPP site from 2013 to 2016.

Section 1) and the measured  $^{137}\text{Cs}$  activity at the 1F NPP harbour to estimate the direct release rate from April 2011 to December 2016. The direct release rates estimated by using the measured  $^{137}\text{Cs}$  activity adjacent to the 1F NPP were generally larger than the rates estimated by using the measured  $^{137}\text{Cs}$  activity in the harbour. The trend of the estimated direct release rate in this study, however, was in good agreement with those estimated by Kanda (2013) and Machida et al. (2019).

### 3.2. River discharge

The river discharge rate of dissolved  $^{137}\text{Cs}$  was obtained by multiplying the flow rate of the river water by the dissolved  $^{137}\text{Cs}$  activity in the river water. The  $^{137}\text{Cs}$  activity of river water was calculated for the 16 rivers listed in Section 2.3.2 by using equation (1), an empirical equation based on the deposited  $^{137}\text{Cs}$  inventory in the basin (Taniguchi et al., 2019). In four rivers (Nakanishi and Sakuma, 2019), the Uda, Ota, Ukedo, and Tomioka rivers (Fig. 4), we compared the estimated dissolved  $^{137}\text{Cs}$  activity with the measured activity. In the Ota and Ukedo rivers, the measured  $^{137}\text{Cs}$  activities were greater than  $100 \text{ Bq m}^{-3}$ . In all four rivers, the measured  $^{137}\text{Cs}$  activities varied seasonally and increased in summer (Tsuzi et al., 2016). The estimated dissolved  $^{137}\text{Cs}$  activities were generally in good agreement with observations, although the estimation method did not take account of the seasonal fluctuations.

The estimated total amount of dissolved  $^{137}\text{Cs}$  from the three rivers around the 1F NPP with large dissolved  $^{137}\text{Cs}$  discharge rates during 2013–2016 was  $3.6 \times 10^{11} \text{ Bq}$  for the Abukuma River,  $3.4 \times 10^{11} \text{ Bq}$  for the Ukedo River, and  $4.3 \times 10^{10} \text{ Bq}$  for the Ota River (Fig. 5). The large discharge rates of these rivers reflect high flow volume, in the case of the Abukuma River, and high dissolved  $^{137}\text{Cs}$  activities, in the case of the Ukedo and Ota rivers. The discharge rates of the other rivers were all below  $1.0 \times 10^{10} \text{ Bq}$ . The total estimated amount of dissolved  $^{137}\text{Cs}$  discharged from all 16 rivers from 2013 to 2016 was  $1.1 \times 10^{12} \text{ Bq}$ , which is an order of magnitude less than the estimated direct release amount during the same period of  $1.4 \times 10^{13} \text{ Bq}$ .

In three major rivers (the Abukuma, Niida, and Ukedo rivers), temporal variabilities of the dissolved  $^{137}\text{Cs}$  discharge rate were large because of large intra-annual variability in the river flow rates (Fig. 6). The dissolved  $^{137}\text{Cs}$  activity decreased exponentially from 2013 to 2016 with an apparent half-life of 2.4 years, but the river flow rates did not exhibit interannual variability. Therefore, the dissolved  $^{137}\text{Cs}$  discharge

rates from the rivers also decreased with an apparent half-life of 2.4 years. In contrast, the direct release rate of dissolved  $^{137}\text{Cs}$  decreased with an apparent half-life of 1 year. On 31 December 2016, the direct release rate was  $1.6 \times 10^9 \text{ Bq day}^{-1}$ , which is an order of magnitude higher than the dissolved  $^{137}\text{Cs}$  discharge rate of the Abukuma and Ukedo rivers of  $1.0 \times 10^8 \text{ Bq day}^{-1}$ .

### 3.3. Flow field

The velocity of the north–south component of current flow along the coast is dominant, whereas that of the east–west flow component is small. We thus compared observed and simulated velocities of the north–south component of the current adjacent to the 1F NPP, and we also examined the velocity difference between simulations with and without river discharges, from 8 October to 10 December 2014, and from 22 April to 25 June 2015 (Fig. 7). The discharges of the Niida, Ota, Ukedo, Kuji, Natui, Okita, Uda, and Tomioka rivers, which are among the 16 rivers closest to the 1F NPP, are also shown in Fig. 7. The simulation reproduced well the dominant north–south flow component and the change in current direction every 3–4 days. In addition, the strengthening of the southward current by the inflow of freshwater from the rivers was reproduced for days when river discharge was relatively large and current velocity was southward (14–17 October 2014, 31 October to 7 November 2014, 25–27 November 2014), although the enhancement of the southward current was small. In other words, the effect of the freshwater flux on the simulated ocean current adjacent to the 1F NPP was small because the river flow rates from the second-class rivers in the vicinity of the 1F NPP were small. Simulated current velocities both with and without rivers were in good agreement with observation.

### 3.4. Temporal change of $^{137}\text{Cs}$ activity

Fig. 8 compares  $^{137}\text{Cs}$  activities measured at the 5,6 discharge and south discharge canals with simulated  $^{137}\text{Cs}$  activities adjacent to the 1F NPP site from 26 March 2011 to 31 December 2016. Simulated  $^{137}\text{Cs}$  activities attributable to direct release were in good agreement with measured activities because the direct release rate was tweaked by the  $^{137}\text{Cs}$  activities measured at these points. Simulated  $^{137}\text{Cs}$  activities varied by one order of magnitude at short time scales because of oceanic

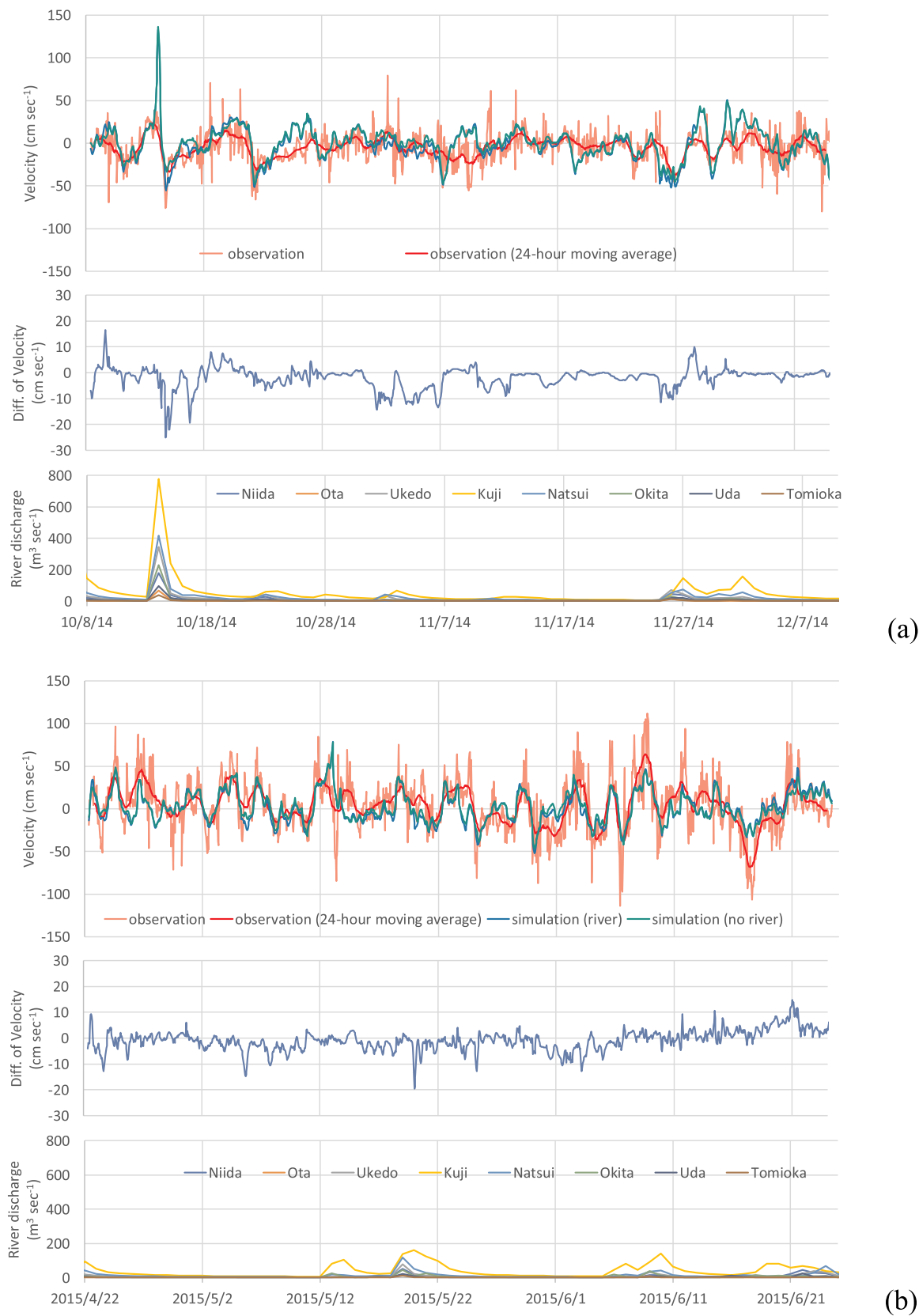


**Fig. 7.** Simulated current velocities, with and without river discharges, compared with the current velocity observed by ADCP adjacent to the 1F NPP (top), differences of velocity between simulations with and without rivers (middle), and discharges of rivers adjacent to the 1F NPP (bottom) from (a) 8 October to 10 December 2014 and (b) 22 April to 25 June 2015.

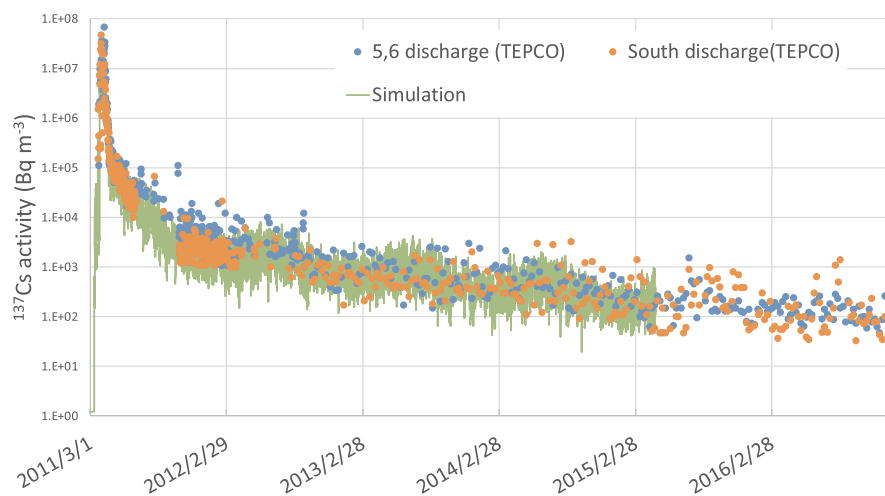


**Fig. 8.** Measured  $^{137}\text{Cs}$  activities at the 5–6 (north) and south discharge canals near the 1F NPP and simulated  $^{137}\text{Cs}$  activities in the mesh adjacent to the 1F NPP site.

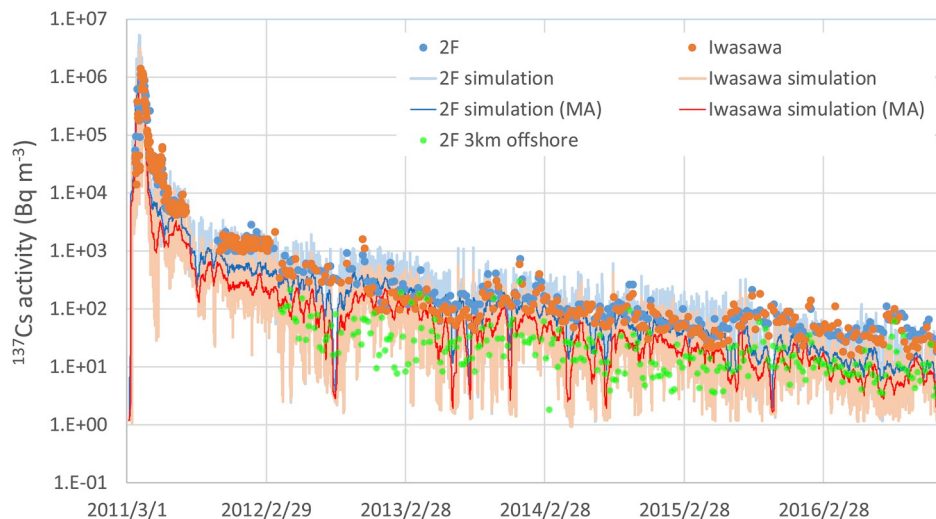


**Fig. 9.** Measured  $^{137}\text{Cs}$  activities at the 2F NPP north discharge canal (10 km south of the 1F NPP site), 3 km offshore of the 2F NPP, and offshore of Iwasawa (16 km south of the 1F NPP site), and simulated  $^{137}\text{Cs}$  activities at the 2F NPP and at Iwasawa. The thick lines show the simulation results, and the thin lines show the 14-day moving average (MA) of the simulation results.

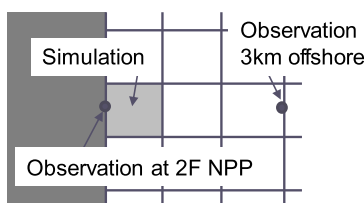


**Fig. 10.** Schematic map showing the locations of the observation points at the 2F NPP and 3 km offshore of the 2F NPP, and the simulation mesh at the 2F NPP.

current changes, even though the temporal variability of the estimated direct release rate was small. The temporal variability of simulated  $^{137}\text{Cs}$  activities attributable to direct release was also in good agreement with the temporal variability of measured activities; this result implies that the estimated direct release rate is reasonable.

Fig. 9 shows measured and simulated  $^{137}\text{Cs}$  activities at the Fukushima Dai-ni Nuclear Power Plant (2F NPP), at a point 3 km offshore of 2F NPP, and offshore of Iwasawa. The 2F NPP and the

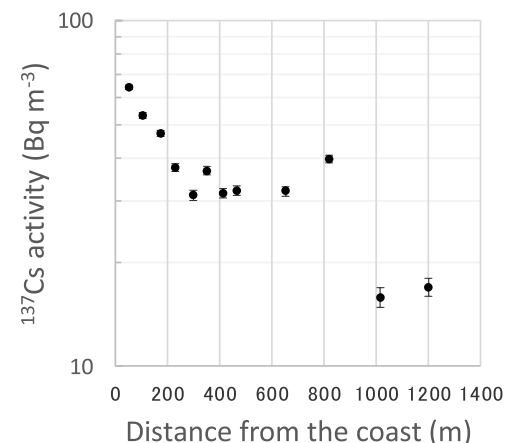


**Fig. 11.** Measured  $^{137}\text{Cs}$  activities offshore of the Tomioka port on 29 August 2014 along  $37^{\circ}20.14'\text{N}$ .

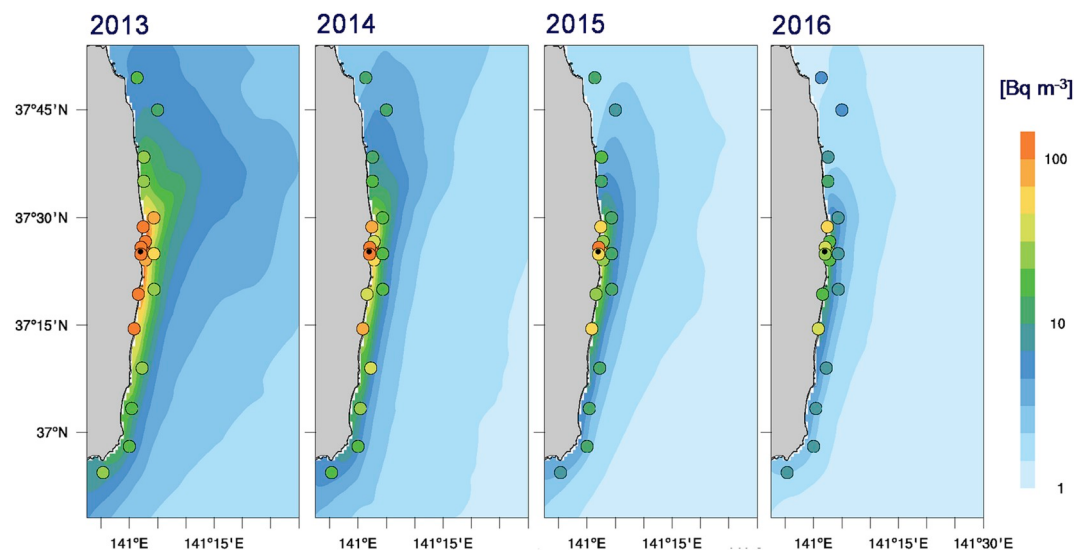


Fig. 12. Annual averaged measured and simulated surface  $^{137}\text{Cs}$  activity in the nearshore region adjacent to the 1F NPP in 2013, 2014, 2015, and 2016.

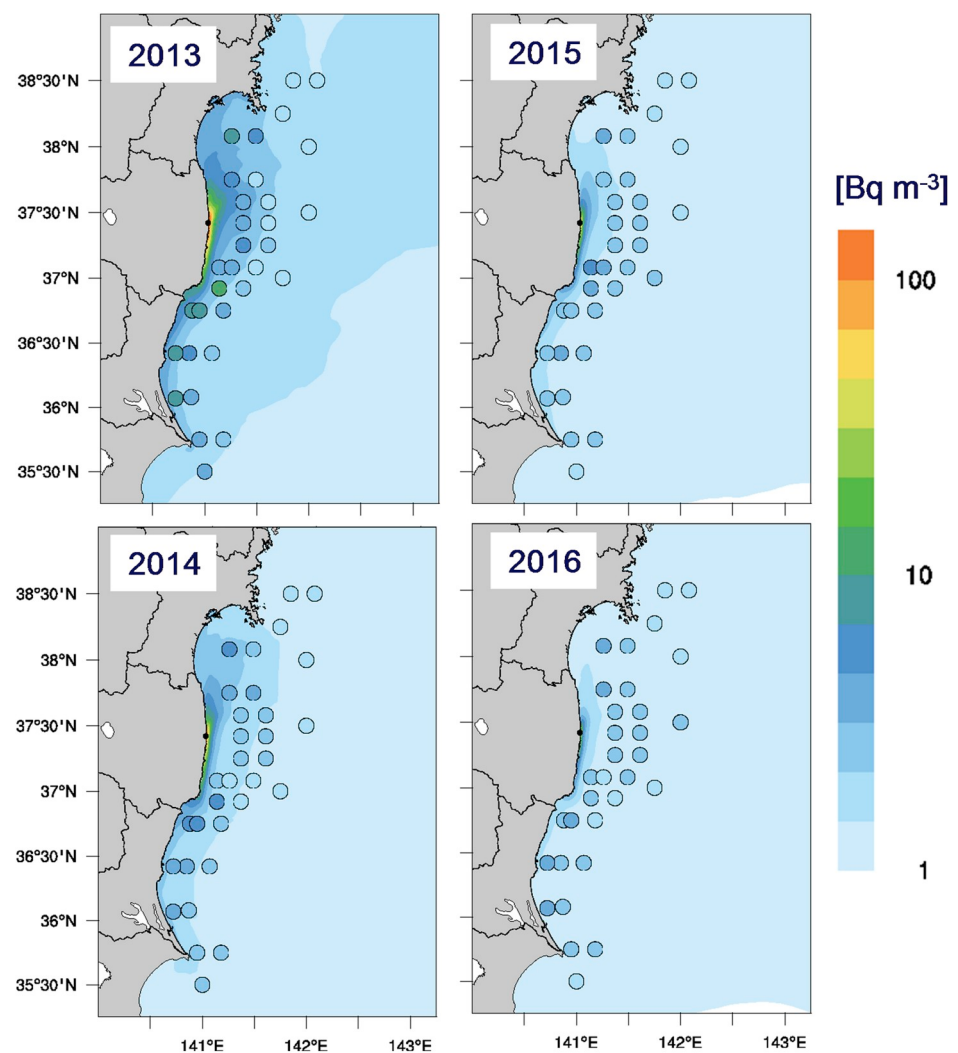
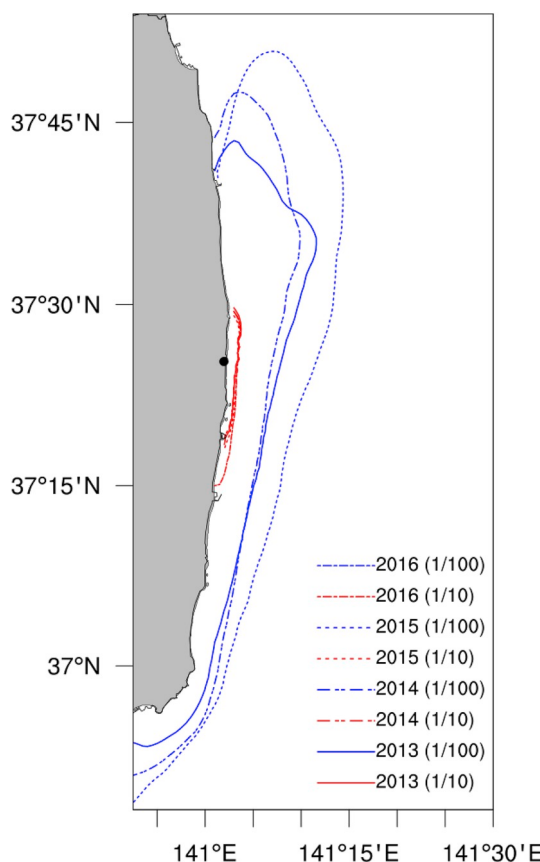


Fig. 13. Annual averaged measured and simulated surface  $^{137}\text{Cs}$  activity in the offshore region during 2013, 2014, 2015, and 2016.



**Fig. 14.** Annual averaged distribution of  $^{137}\text{Cs}$  activity normalized by the maximum  $^{137}\text{Cs}$  activity in front of the 1F NPP site. Red lines show the 1/10 contours, and blue lines show the 1/100 contours for each year. The 1/100 contour for 2016 is missing because the  $^{137}\text{Cs}$  activity in that year was less than the background  $^{137}\text{Cs}$  activity of  $1 \text{ Bq m}^{-3}$ . (For interpretation of the references to colour in this figure legend, the reader is referred to the Web version of this article.)

Iwasawa coast are located 10 km and 16 km south of the 1F NPP, respectively. Although the temporal trends of the simulated and measured  $^{137}\text{Cs}$  activities were in good agreement, simulated  $^{137}\text{Cs}$  activities were underestimated compared to the measured activities. The 2F NPP and Iwasawa coast sampling points were immediately adjacent to the coast, whereas the simulation estimated the averaged  $^{137}\text{Cs}$  activity in one simulation mesh (about  $1 \text{ km} \times 1 \text{ km}$ ) (Fig. 10). Fig. 11 shows  $^{137}\text{Cs}$  activities measured off Tomioka port, which is located between the 1F NPP and the 2F NPP, on 29 August 2014. The samples were collected at 100–200 m intervals along a transect ( $\sim 1 \text{ km}$  long) normal to the coast. The measured  $^{137}\text{Cs}$  activity decreased exponentially over a distance of  $\sim 1 \text{ km}$  in an offshore direction from the coast (i.e., sub-grid scale). Therefore, the simulated  $^{137}\text{Cs}$  activities were generally smaller than the measured activities. Moreover, they were between those measured at the 2F NPP discharge canal and those measured 3 km offshore of the 2F NPP. A model simulation at finer resolution would thus be necessary to represent the detailed activity distribution along the coast. In addition, waves can also affect nearshore material transport. The  $^{137}\text{Cs}$  activities measured at the 2F NPP and at Iwasawa peaked in summer (Fig. 9). These peaks may reflect a change in the direct release rate, or one in the transport process from the 1F NPP to the 2F NPP and Iwasawa coast, or both. The simulated  $^{137}\text{Cs}$  activities at the 2F NPP and Iwasawa coast, however, did not show corresponding peaks, even though the model can represent the transport process along the coast well (Tsumune et al., 2012). Thus, the peaks in the measured  $^{137}\text{Cs}$  activity in summer may be due to a change in the direct release rate.

Precipitation increases in summer in the Fukushima area, so the seasonal change in the direct release rate might be related to precipitation changes. In this study, we did not consider seasonal changes in our estimation of the direct release rate, but it may be important for the one after 2017 for a future study.

### 3.5. Annual average

We examined the accuracy of the simulated surface  $^{137}\text{Cs}$  activity distribution from 2013 to 2016. During that period, the direct leakage rate was decreasing exponentially, and surface  $^{137}\text{Cs}$  activity offshore was not influenced by atmospheric deposition. Surface  $^{137}\text{Cs}$  activity distributions were spatially heterogeneous, however, and they also fluctuated temporally because of surface wind and mesoscale eddy changes. Therefore, to evaluate the accuracy of the simulation, we calculated the annual averaged surface  $^{137}\text{Cs}$  activities and then compared nearshore (Fig. 12) and offshore (Fig. 13) annual averaged measured surface  $^{137}\text{Cs}$  activities with the simulated nearshore and offshore activities, respectively, without river discharge in 2013, 2014, 2015, and 2016. In this comparison, we used archived measurement data from TEPCO (<http://www.tepco.co.jp/en/nu/fukushima-np/f1/smp/index-e.html>) and the Nuclear Regulation Authority (<https://radioactivity.nsr.go.jp/en/>) and data published by Takata et al. (2016). As  $^{137}\text{Cs}$  is transported southward, it spreads along the coast under the influence of the Coriolis force. In contrast, when  $^{137}\text{Cs}$  is advected northward, it spreads toward the northeast, away from the coast, as a result of shelf wave propagation. Fig. 14 shows the annual averaged distribution of simulated  $^{137}\text{Cs}$  activity normalized by the maximum  $^{137}\text{Cs}$  activity in the release mesh adjacent to the 1F NPP site. The distribution patterns were similar among the years even though reanalysis data of each year were employed as the driving force of the ROMS. This result indicates that the interannual variability of surface  $^{137}\text{Cs}$  activity distribution is small in this area. Therefore, if information on the release rate is available, the annual averaged  $^{137}\text{Cs}$  activity distribution should be predictable by this simulation.

The results of the comparison between nearshore and offshore measured and simulated surface  $^{137}\text{Cs}$  activities in 2013, 2014, 2015, and 2016 (Fig. 15) showed that the simulated results were generally in good agreement with observations. The simulated results for 2015 and 2016 were underestimated compared with the observation in the area where  $^{137}\text{Cs}$  activity was less than  $10 \text{ Bq m}^{-3}$ . The cause of this underestimation was not underestimation of the direct release rate, but it is possible that inflow of  $^{137}\text{Cs}$  across the domain boundary due to recirculation in the North Pacific was underestimated. The effect of such inflow of  $^{137}\text{Cs}$  derived from the 1F NPP accident was negligible one year after the 1F NPP accident (Tsumune et al., 2013), but recent studies have shown that  $^{137}\text{Cs}$  activity along the Japanese coast increased after 2012 as a result of recirculation in the North Pacific (Aoyama et al., 2017; Inomata et al., 2018). The North Pacific model which were used to represent inflow across the ROMS domain boundary, did not reproduce recirculation processes around the Japanese coast, therefore this model result did not reflect  $^{137}\text{Cs}$  derived from recirculation (Tsubono et al., 2016).

In the comparison between measured and nearshore surface  $^{137}\text{Cs}$  activity simulated with and without river discharge in 2013, 2014, 2015, and 2016 (Fig. 16), the surface  $^{137}\text{Cs}$  activities simulated with river discharge were not very different from those simulated without river discharge, although surface  $^{137}\text{Cs}$  activities simulated with river discharge were slightly smaller than those simulated without river discharge at some points because of oceanic current changes. This result implies that direct release was dominant in comparison with river discharge as a source of oceanic surface  $^{137}\text{Cs}$  activity. The apparent half-life of directly released  $^{137}\text{Cs}$  (346 days), however, was shorter than that of the river discharge (2.4 years), so it is likely that an effect of river discharge on oceanic  $^{137}\text{Cs}$  activity will be detected in the future even though the  $^{137}\text{Cs}$  activity will be very low.

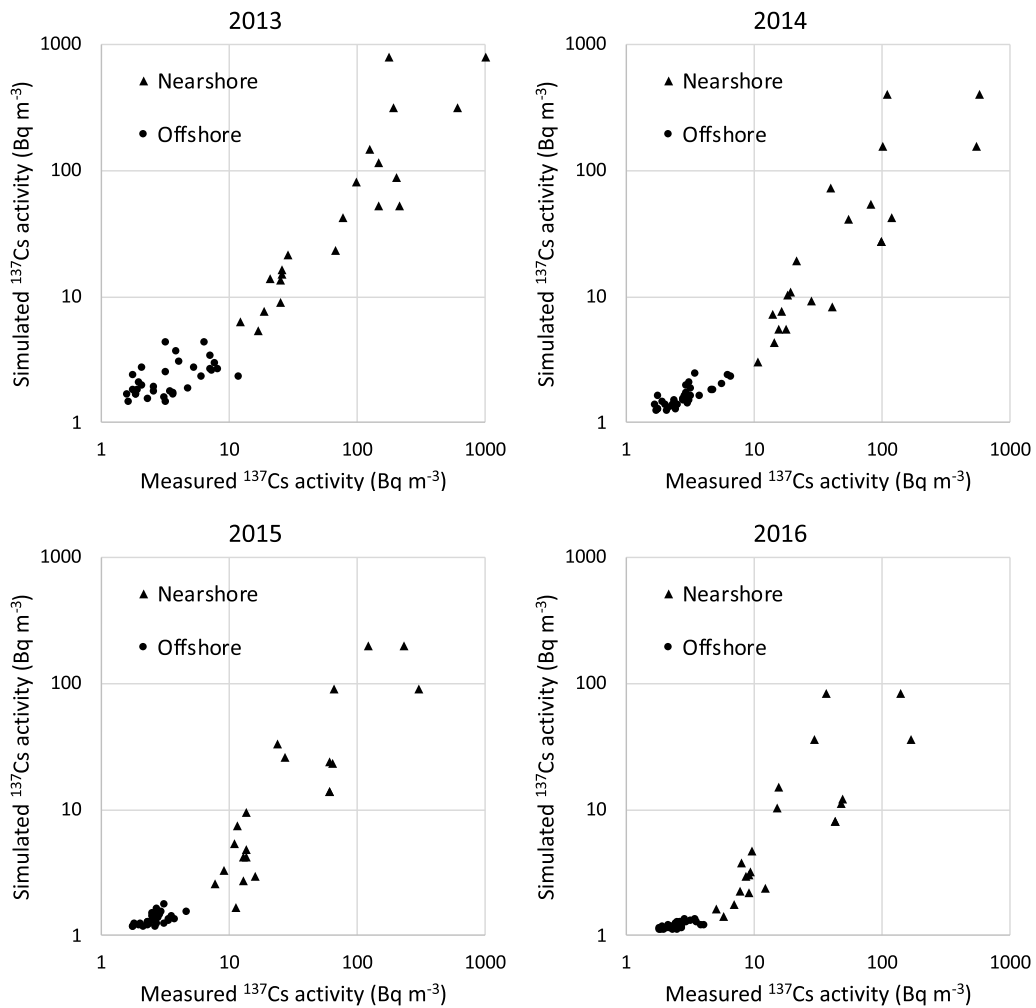


**Fig. 15.** Comparison between measured and simulated surface  $^{137}\text{Cs}$  activities in the nearshore and offshore regions.

Annual direct release of  $^{137}\text{Cs}$ , annual river discharge of  $^{137}\text{Cs}$ , annual averaged  $^{137}\text{Cs}$  inventory in the model domain are summarized in Table 1. The annual direct releases of  $^{137}\text{Cs}$  were larger than the annual river discharge from 2013 to 2014. The volume of the model domain is about  $2.69 \times 10^{14} \text{ m}^3$ . Annual averaged inventory in the model domain was affected by direct release in 2011. After 2013, direct release and river discharge did not increase the annual averaged  $^{137}\text{Cs}$  inventory in the model domain. The annual averaged  $^{137}\text{Cs}$  inventory was affected by the background  $^{137}\text{Cs}$  activity derived from global fallout due to atmospheric weapons tests before the 1F NPP accident.

#### 4. Summary

The estimated direct release rate of  $^{137}\text{Cs}$  from 26 March 2011 to 31 December 2016 was initially  $2.2 \times 10^{14} \text{ Bq day}^{-1}$ , and it decreased exponentially with time, reaching  $3.9 \times 10^9 \text{ Bq day}^{-1}$  by the end of 2016. After November 2011, the direct release rate decreased exponentially with an apparent half-life of about 1 year. The total leakage during the first year was estimated to be  $3.6 \pm 0.7 \text{ PBq}$ , and the estimated total leakage remained the same after 6 years. The total estimated amount of dissolved  $^{137}\text{Cs}$  discharged from 16 rivers from 2013 to 2016

was  $1.1 \times 10^{12} \text{ Bq}$ , which is an order of magnitude less than the total amount of directly released  $^{137}\text{Cs}$  ( $1.4 \times 10^{13} \text{ Bq}$ ) during the same period.

We employed the Regional Ocean Model System (ROMS) to simulate the dissolved  $^{137}\text{Cs}$  activity considering as sources direct release, river discharge, and inflow across the domain boundary. Simulated  $^{137}\text{Cs}$  activities attributable to direct release were in good agreement with measured activities, a result that implies that the estimated direct release rate is reasonable. The simulated annual averaged distributions of surface  $^{137}\text{Cs}$  activity was in good agreement with observations conducted from 2013 to 2016 and were similar among the years; therefore, the distribution should be predictable by the simulation provided that information on the release rate is available. The simulated results were underestimated compared with observations in the area where  $^{137}\text{Cs}$  activity was less than  $10 \text{ Bq m}^{-3}$  in 2015 and 2016. The cause of this underestimation is not underestimation of the direct release, but inflow across the domain boundary due to recirculation in the North Pacific may have been underestimated. No effect of river discharge of  $^{137}\text{Cs}$  on oceanic  $^{137}\text{Cs}$  distributions was detected because the effect of direct release remained dominant during the study period.

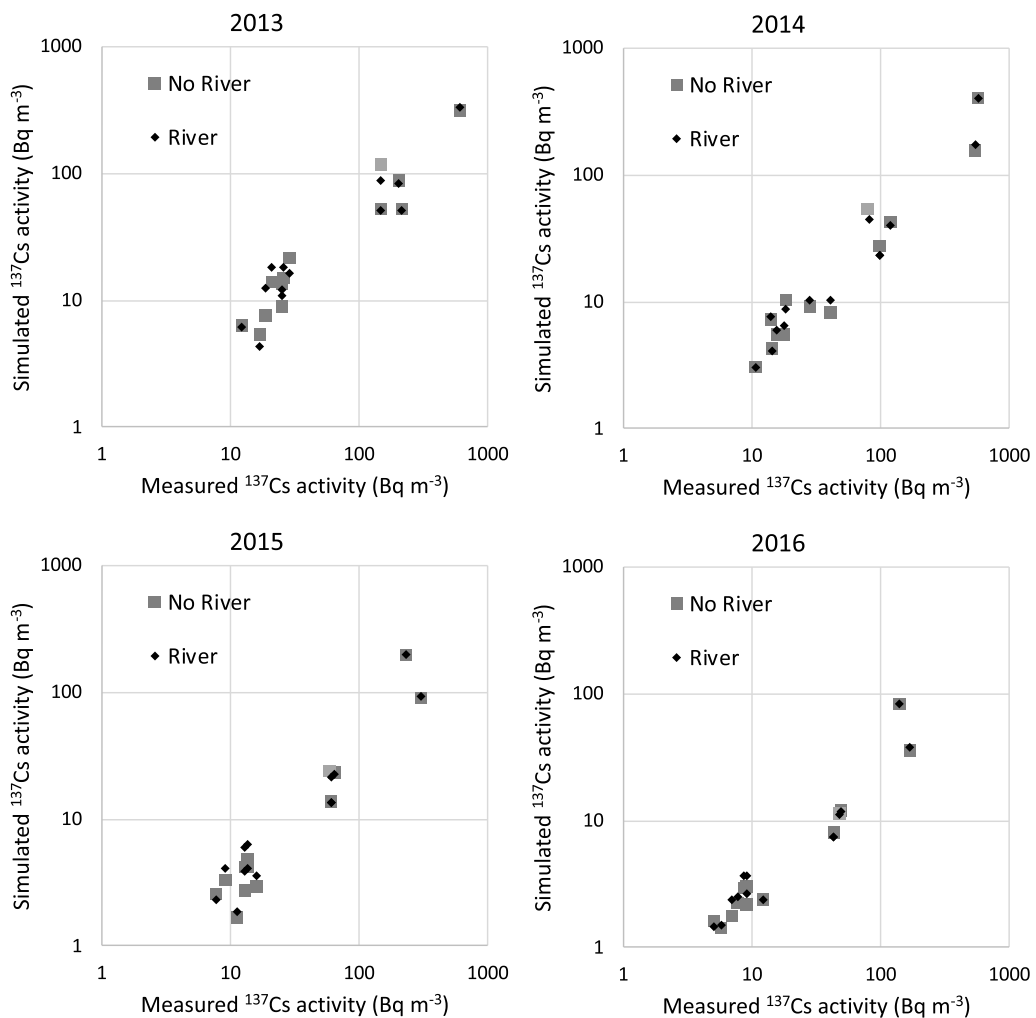


**Fig. 16.** Comparison of observed nearshore surface  $^{137}\text{Cs}$  activities with those simulated with and without river discharge.

**Table 1**

Annual amounts of  $^{137}\text{Cs}$  directly released into the ocean and discharged from rivers during 2011–2016.

Year	Direct release (Bq year <sup>-1</sup> )	River discharge (Bq year <sup>-1</sup> )	Annual averaged inventory in the model domain (Bq year <sup>-1</sup> )	
			No river	River
2011	$3.55 \times 10^{15}$	?	$3.30 \times 10^{15}$	?
2012	$1.63 \times 10^{13}$	?	$6.10 \times 10^{14}$	?
2013	$7.81 \times 10^{12}$	$3.53 \times 10^{11}$	$3.02 \times 10^{14}$	$3.02 \times 10^{14}$
2014	$3.76 \times 10^{12}$	$3.55 \times 10^{11}$	$2.64 \times 10^{14}$	$2.65 \times 10^{14}$
2015	$1.81 \times 10^{12}$	$2.28 \times 10^{11}$	$2.46 \times 10^{14}$	$2.46 \times 10^{14}$
2016	$8.75 \times 10^{11}$	$1.48 \times 10^{11}$	$2.29 \times 10^{14}$	$2.29 \times 10^{14}$

#### Declaration of competing interest

The authors declare that they have no known competing financial interests or personal relationships that could have appeared to influence the work reported in this paper.

#### Acknowledgments

We thank Fukiko Taguchi, Ryosuke Niwa, and Kaori Miyata for their technical help with the model simulations. We also thank Takashi Ishimaru, Yoshiaki Maeda, and Yoshinori Sato for their ocean current observations. This study was conducted mainly with support from the in-laboratory research fund of the Central Research Institute of the Electric Power Industry (CRIEPI). This research was also supported by a Grant-in-Aid for Scientific Research on Innovative Areas, “Interdisciplinary study on environmental transfer of radionuclides from the Fukushima Dai-ichi NPP Accident” (project no. 25110511) from the Japanese Ministry of Education, Culture, Sports, Science and Technology (MEXT).

#### Appendix A. Supplementary data

Supplementary data to this article can be found online at <https://doi.org/10.1016/j.jenvrad.2020.106173>.

#### References

- Aoyama, M., Hirose, K., 2008. Radiometric determination of anthropogenic radionuclides in seawater. In: Pavel, P.P. (Ed.), Radioactivity in the Environment. Elsevier, Oxford, pp. 137–162. [https://doi.org/10.1016/S1569-4860\(07\)11004-4](https://doi.org/10.1016/S1569-4860(07)11004-4).

- Aoyama, M., Hamajima, Y., Inomata, Y., Oka, E., 2017. Recirculation of FNPP1-derived radiocaesium observed in winter 2015/2016 in coastal regions of Japan. *Appl. Radiat. Isot.* 126, 83–87.
- Aoyama, M., Kajino, M., Tanaka, T.Y., Sekiyama, T.T., Tsumune, D., Tsubono, T., Hamajima, Y., Inomata, Y., Gamo, T., 2016.  $^{134}\text{Cs}$  and  $^{137}\text{Cs}$  in the north Pacific Ocean derived from the March 2011 TEPCO Fukushima Dai-ichi nuclear power plant accident, Japan. Part two: estimation of  $^{134}\text{Cs}$  and  $^{137}\text{Cs}$  inventories in the north Pacific Ocean. *J. Oceanogr.* 72, 67–76.
- Estournel, C., Bosc, E., Bocquet, M., Ulses, C., Marsaleix, P., Winiarek, V., Osvath, I., Nguyen, C., Duham, T., Lyard, F., Michaud, H., Auclair, F., 2012. Assessment of the amount of cesium-137 released into the Pacific Ocean after the Fukushima accident and analysis of its dispersion in Japanese coastal waters. *J. Geophys. Res.* 117.
- Hashimoto, A., Hirakuchi, H., Toyoda, Y., Nakaya, K., 2010. Prediction of regional climate change over Japan due to global warming (Part 1) e Evaluation of numerical weather forecasting and analysis system (NuWFAS) applied to a long-term climate simulation. CRIEPI report, p. N10044 (in Japanese).
- Inomata, Y., Aoyama, M., Hamajima, Y., Yamada, M., 2018. Transport of FNPP1-derived radiocaesium from subtropical mode water in the western North Pacific Ocean to the Sea of Japan. *Ocean Sci.* 14, 813–826.
- Japanese Government, 2011. Report of Japanese Government to the IAEA Ministerial Conference on Nuclear Safety – the Accident at TEPCO's Fukushima Nuclear Power Stations. [https://japan.kantei.go.jp/kan/topics/201106/iaea\\_houkokusho\\_e.html](https://japan.kantei.go.jp/kan/topics/201106/iaea_houkokusho_e.html). (Accessed 15 January 2020).
- Kakehi, S., Kaeriyama, H., Ambe, D., Ono, T., Ito, S.I., Shimizu, Y., Watanabe, T., 2015. Radioactive cesium dynamics derived from hydrographic observations in the Abukuma River Estuary, Japan. *J. Environ. Radioact.* 153, 1–9.
- Kamidaira, Y., Uchiyama, Y., Kawamura, H., Kobayashi, T., Furuno, A., 2018. Submesoscale mixing on initial dilution of radionuclides released from the Fukushima Daiichi nuclear power plant. *J. Geophys. Res.: Oceans* 123, 2808–2828.
- Kanda, J., 2013. Continuing  $^{137}\text{Cs}$  release to the sea from the Fukushima Dai-ichi nuclear power plant through 2012. *Biogeosciences* 10, 6107–6113.
- Kitamura, A., Yamaguchi, M., Kurikami, H., Yui, M., Onishi, Y., 2014. Predicting sediment and cesium-137 discharge from catchments in eastern Fukushima. *Anthropocene* 5, 22–31.
- Kumamoto, Y., Yamada, M., Aoyama, M., Hamajima, Y., Kaeriyama, H., Nagai, H., Yamagata, T., Murata, A., Masumoto, Y., 2019. Radiocaesium in North Pacific coastal and offshore areas of Japan within several months after the Fukushima accident. *J. Environ. Radioact.* 198, 79–88.
- Machida, M., Yamada, S., Iwata, A., Otosaka, S., Kobayashi, T., Watanabe, M., Funasaka, H., Morita, T., 2019. Seven-year temporal variation of cesium-137 discharge inventory from the port of Fukushima Dai-ichi nuclear power plant. *Trans. Atom. Energy Soc. Jpn.* 18, 226–236. J18.030. (in Japanese).
- Maderich, V., Bezhnar, R., Heling, R., de With, G., Jung, K.T., Myoung, J.G., Cho, Y.K., Qiao, F., Robertson, L., 2014. Regional long-term model of radioactivity dispersion and fate in the Northwestern Pacific and adjacent seas: application to the Fukushima Dai-ichi accident. *J. Environ. Radioact.* 131, 4–18.
- Maderich, V., Bezhnar, R., Tateda, Y., Aoyama, M., Tsumune, D., 2018. Similarities and differences of  $^{137}\text{Cs}$  distributions in the marine environments of the Baltic and Black sea and off the Fukushima Dai-ichi nuclear power plant in model assessments. *Mar. Pollut. Bull.* 135, 895–906.
- Masumoto, Y., Miyazawa, Y., Tsumune, D., Tsubono, T., Kobayashi, T., Kawamura, H., Estournel, C., Marsaleix, P., Lanerolle, L., Mehra, A., Garraffo, Z.D., 2012. Oceanic dispersion simulations of  $^{137}\text{Cs}$  released from the Fukushima Daiichi nuclear power plant. *Elements* 8, 207–212.
- Miyazawa, Y., Masumoto, Y., Varlamov, S.M., Miyama, T., Takigawa, M., Honda, M., Saino, T., 2013. Inverse estimation of source parameters of oceanic radioactivity dispersion models associated with the Fukushima accident. *Biogeosciences* 10, 2349–2363.
- Miyazawa, Y., Zhang, R., Guo, X., Tamura, H., Ambe, D., Lee, J.-S., Okuno, A., Yoshihara, H., Setou, T., Komatsu, K., 2009. Water mass variability in the western North Pacific detected in a 15-year eddy resolving ocean reanalysis. *J. Oceanogr.* 65, 737–756.
- Nakanishi, T., Sakuma, K., 2019. Trend of  $^{137}\text{Cs}$  concentration in river water in the medium term and future following the Fukushima nuclear accident. *Chemosphere* 215, 272–279.
- Sanada, Y., Urabe, Y., Sasaki, M., Ochi, K., Torii, T., 2018. Evaluation of ecological half-life of dose rate based on airborne radiation monitoring following the Fukushima Dai-ichi nuclear power plant accident. *J. Environ. Radioact.* 192, 417–425.
- Science Council of Japan, 2014. A Review of the Model Comparison of Transportation and Deposition of Radioactive Materials Released to the Environment as a Result of the Tokyo Electric Power Company's Fukushima Daiichi Nuclear Power Plant Accident report. <http://www.scj.go.jp/ja/info/kohyo/pdf/kohyo-22-h140902-e1.pdf>. (Accessed 8 October 2019).
- Shchepetkin, A.F., McWilliams, J.C., 2005. The regional oceanic modeling system (ROMS): a split-explicit, free-surface, topography-following-coordinate oceanic model. *Ocean Model.* 9, 347–404.
- Skamarock, W.C., Klemp, J.B., Dudhia, J., Gill, D.O., Barker, D.M., Duda, M., Huang, H., Wang, W., Powers, J.G., 2008. A description of the advanced research WRF version 3. NCAR Tech. Note NCAR/TN-475+STR, p. 113.
- Taniguchi, K., Onda, Y., Smith, H.G., Blake, W.H., Yoshimura, K., Yamashiki, Y., Kuramoto, T., Saito, K., 2019. Transport and redistribution of radiocaesium in Fukushima fallout through rivers. *Environ. Sci. Technol.* 53, 12339–12347.
- Takata, H., Kusakabe, M., Inatom, N., Ikenoue, T., Hasegawa, K., 2016. The contribution of sources to the sustained elevated inventory of  $^{137}\text{Cs}$  in offshore waters east of Japan after the Fukushima Dai-ichi nuclear power station accident. *Environ. Sci. Technol.* 50, 6957–6963.
- Toyoda, Y., Hirakuchi, H., 2009. Development of Hydrological Model with Meteorological Forecast Model - an Application to Typhoon Case Attacked to a Kyushu District -, CRIEPI report, p. N08058 (in Japanese).
- Tsubono, T., Misumi, K., Tsumune, D., Bryan, F.O., Hirose, K., Aoyama, M., 2016. Evaluation of radioactive cesium impact from atmospheric deposition and direct release fluxes into the North Pacific from the Fukushima Daiichi nuclear power plant. *Deep Sea Res. Oceanogr. Res. Pap.* 115, 10–21.
- Tsuji, H., Nishikiori, T., Yasutaka, T., Watanabe, M., Ito, S., Hayashi, S., 2016. Behavior of dissolved radiocaesium in river water in a forested watershed in Fukushima prefecture. *J. Geophys. Res.: Biogeosciences* 121, 2588–2599.
- Tsumune, D., Tsubono, T., Aoyama, M., Hirose, K., 2012. Distribution of oceanic  $^{137}\text{Cs}$  from the Fukushima Dai-ichi Nuclear Power Plant simulated numerically by a regional ocean model. *J. Environ. Radioact.* 111, 100–108.
- Tsumune, D., Tsubono, T., Aoyama, M., Uematsu, M., Misumi, K., Maeda, Y., Yoshida, Y., Hayami, H., 2013. One-year, regional-scale simulation of  $^{137}\text{Cs}$  radioactivity in the ocean following the Fukushima Dai-ichi Nuclear Power Plant accident. *Biogeosciences* 10, 5601–5617.